J. Nanoanalysis., 5(3): 143-155 Summer 2018

ORIGINAL RESEARCH PAPER

Adsorption of malachite green dye on different natural absorbents modified with magnetite nanoparticles

Naereh Besharati, Nina Alizadeh*

Department of Chemistry, University of Guilan, Rasht, Iran

Received: 2018-03-16 Accepted: 2018-05-20 Published: 2018-08-10

ABSTRACT

This study was focused on the adsorption of malachite green as a cationic dye on magnetite nanoparticles loaded green tea waste (MNLGTW), peanut husk (MNLPH), Azolla (MNLA) and Fig leave (MNLFL) as naturally cheap sources of adsorbent. MNLGTW, MNLPH, MNLA and MNLFL were prepared with chemical precipitation method and they were characterized with Fourier transform infrared spectroscopy (FT-IR), powder X-ray diffraction (XRD), Scanning electron microscopy (SEM) and Energy Dispersive X- ray (EDX) analysis. Different parameters affecting the dye removal efficiency were optimized. At optimum conditions, the sorption of the malachite green on the MNLGTW, MNLPH, MNLA, and MNLFL adsorbents was best described by a pseudo second-order kinetic model with R^2 =1, $q_{eq= 12.51}$ mg g^{-1} , R^2 =0.9996, $q_{eq=625}$ mg g^{-1} , R^2 =0.9842, $q_{eq=0.5772}$ mg g^{-1} and R^2 =0.9912, $q_{eq=0.517}$ mg g^{-1} respectively. Equilibrium data were fitted well to the Langmuir isotherm more than Freundlich and Temkin isotherm. The synthesized sorbent showed complete dye removal with 112.359, 98.039, 23.1 and 73.2 mg g^{-1} for MNLGTW, MNLPH, MNLA,and MNLFL, respectively. The results showed MNLGTW, MNLPH, MNLA and MNLFL can be used as efficient adsorbents for removal of malachite green from aqueous solutions.

Keywords: *Magnetic Nanoparticles, Malachite Green, Natural Absorbents*

How to cite this article
Besharati N, Alizadeh N. Adsorption of malachite green dye on different natural absorbents modified with magnetite nanoparticles. J. Nanoanalysis., 2018; 5(3): 143-155. DOI: 10.22034/jna.2018.551649.1048

INTRODUCTION

Dyes are used in large quantity in many industries including textile, leather, cosmetics, paper, printing, plastic, pharmaceutical, food, etc. to color their product [1]. Dyes usually have complex aromatic structures which make them stable and difficult to decompose. Malachite green (MG) is a synthetic and organic dye that is used to color fabric and paper. On the other hand, it is also used as a dye in silk, wool, jute, leather, cotton and acrylic industries [2]. Malachite green, a triarylmethane dye is a dark green and crystalline solid form. MG is used as a parasiticide and antibacterial. Residues of MG and its main biotransformation product, leucomalachite green (LMG), may be present in fish that are available for consumption. It has been reported to cause carcinogenesis, mutagenesis, chromosomal fractures, teratogenicity and respiratory toxicity [3-5]. A number of conventional chemical and physical treatment methods have been reported for decolorization of wastewater, including coagulation-flocculation, precipitation, advanced oxidation, ion exchange, membrane filtration, adsorption onto low-cost adsorbents, etc. However, these conventional treatment methods suffer from high cost and inability to meet permissible disposal levels. Sorption has been widely used for the removal of different dyes and other hazardous species from wastewater and it is an economical and efficient method [6]. On the other hand, nanotechnology research and development for the treatment of wastewaters is vital to human beings. These technologies are economical, reliable, rapid and durable to treat wastewaters by eliminating

* Corresponding Author Email: *n–alizadeh@guilan.ac.ir*

specific types of pollutants from water [7]. Different agriculture waste material such as rice husk [8], peanut husk [9,10], coffee [11], sawdust [12], banana pith [13], orange peel [14], wheat straw [15], powdered waste sludge [16], wheat shells [17], wheat bran [18] and hen feathers [19] are used for dye removal and recently, magnetic separation has been applied in many areas to remove, isolate and/or concentrate the desired components from a sample solution. Nanosized magnetic iron oxide particles have been studied extensively as a new adsorbent with the large surface area and small diffusion resistance [20-24]. At present, many methods, such as co-precipitation, microemulsion, thermal decomposition and hydrothermal synthesis, have been applied and reviewed for the production of Fe_3O_4 nanoparticles (NPs) [25]. Among these methods, co-precipitation is a facile method that synthesizes iron oxides from aqueous Fe^{2+}/ Fe^{3+} salt solutions [26,27]. So, this study focused on green tea waste and peanut husk modified with magnetite iron oxide nanoparticles as adsorbents for the removal of malachite green.

Historically, Lahijan is the first town in Iran to have tea plantations; Lahijan stands to have the largest area of tea cultivation with its mild weather, soil quality, and fresh spring water. So tea is available in huge amount and also it is economical to use as an adsorbent of dye. Peanut production in the world is 34.4 billion kg/year [28]. Peanut in Iran is planted in Golestan, Khuzestan and Guilan provinces. In Guilan province, it is planted mainly in Astaneh Ashrafieh city [29]. Skin will be separated for processing of peanuts, so a lot of peanut husk is available.

To produce green tea, leaves are harvested, withered, and then heated through steaming (Japanese style) or pan-firing (Chinese style). This process halts oxidation so the leaves retain their color and delicate, fresh flavor. To produce black tea; leaves are harvested and withered and then crushed, torn, curled, or rolled and allowed to oxidize before being dried. As a result,the leaves darken and develop a stronger flavor and aroma [30]. Azolla grows in paddy fields and Fishponds and Fig leave found in abundance in Iran.

In order to continue our recent work [31], the aim of this research is usability of magnetic nanoparticles loaded green tea waste (MNLTW), peanut husk (MNLPH), Azolla (MNLA) and Fig leave (MNLFL) for malachite green removal of wastewater and two kinetic models were examined. Optimum conditions, kinetic and thermodynamic study were evaluated to obtain the highest dye removal capacity.

EXPERIMENTAL

All used reagents were of analytical reagent grade with the highest purity. Malachite green as cationic dye was obtained from Merck (Darmstadt, Germany). Ferric chloride hexahydrate ($FeCl_3.6H_2O$), ferrous chloride tetrahydrate ($FeCl_2.4H_2O$), amonia, hydrochloric acid, sodium chloride and sodium hydroxide were prepared from Merck. Stock solutions of malachite green were prepared by solving a certain amount of color in distilled water. The molecular structure of malachite green is shown in Fig 1. These solutions were used for optimization of effective parameters and also for planning calibration curve in order to calculate the dye removal efficiency with the spectrophotometer. All stock and working solutions were prepared by using double distilled water.

A Jenway pHmeter (model 370, England) was used for pH measurements. All of the spectrophotometric measurements of dye in the solutions were done at its λ_{max} (620 nm) with a single beam spectrophotometer Jenway model 6105 (England). SEM images were obtained using digital scanning electron microscope (SEM) (model EM3200, USA). X-ray diffractometer (XRD) (model Xpert MPD, Philips, Holland) using CU K_α radiation source with the 2θ range of 0.5-70°, was used for determining of crystal phases and crystallinity of synthesized materials. The infrared spectra of pretreated tea waste and MNLTW were recorded in the wave number range of 400-4000cm^{-1} by Bruker Fourier transform infrared spectrophotometer (FT-IR model Alfa, Germany).

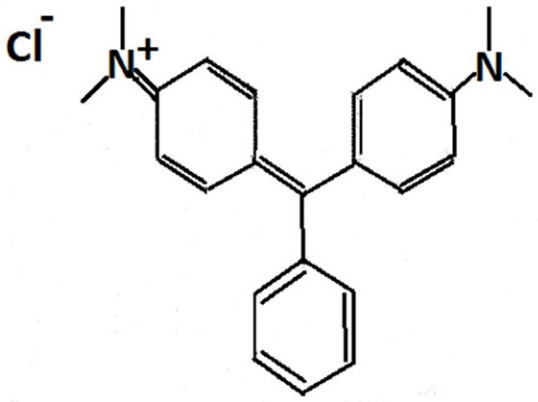

Fig. 1. Chemical structure of malachite green

Coffee Grinder (model MCG 1575) was used for grinding of green tea waste and rotator (model IKA Ms 3 basic, Germany) was used for mixing. For magnetic separation, a strong super magnet (1×3×5cm)with 1.4 T magnetic field was applied.

Preparation of the adsorbents

Green tea waste leaves were produced by Timen Company of Refah Lahijan. Green tea waste leaves were washed with water and then distilled water (3 times) to remove all the dirt particles. For remove caffeine, tannin and color from tea, it boiled with distilled water at 80ºC for 1 h and then washed with distilled water until the washing water contained no color. Green tea waste was dried in an oven at 100ºC for 10 h. The dried tea was then crushed and sieved (with a stainless steel strainer (100 µm) and almost 30% of crushed green tea wastes was retained) and stored in a bottle [31].

Peanut husk was collected from Astaneh Ashrafieh city; its salt was removed by washing with water(three times) and then peanut husk was dried in the oven at 100ºC for 1 h. The husk was milled in a coffee mill and fraction smaller than 0.5 mm was collected and used for magnetic modification. Azolla filiculoides were obtained from fish ponds in Keshelvarzal, Rasht, Iran. The Azolla was washed with water and dried in sun. They were then powdered and sieved for using as a biosorbent and dried in oven at 100ºC and milled in a coffee mill and fraction smaller than 0.5 mm were stored for magnetic modification [32].

Fig leaves were obtained from Rasht, Iran. 10 g of Fig leaves were agitated in 2 L of distilled water in a beaker vigorously (at a speed of 40 rpm) by a magnetic stirrer at ambient temperature of 25 ± 1°C during 4 h, then filtered, continuously washed with distilled water to remove the surface adhered particles and water-soluble materials, and oven-dried at 80°C for 24 h after filtration. These materials were crushed and sieved to (> 0.125 mm), for further batch sorption experiments [33].

Preparation of magnetic nanoparticles loaded Azolla and Fig leaves

Magnetite nanoparticles loaded Azolla (MNLA) and magnetite nanoparticles loaded Fig leaves (MNLFL) were synthesized according to the following procedure: $FeCl_3.6H_2O$ (6.1 g) and $FeSO_4.4H_2O$ (4.2 g) were dissolved in 100 mL distilled water and heated to 90 °C. 10 mL of ammonium hydroxide (28%) and the suspensions of 1 g of Azolla powder (for preparation of MNLA) and 1 g of Fig leaves (for preparation of MNLFL) were dissolved in 200 mL of distilled water and were added rapidly to prepared Fe^{2+}/Fe^{3+} solution. The pH of the reaction medium was adjusted to 10. The mixture was stirred at 80 °C for 30 min and then cooled to room temperature. The black precipitate Fe_3O_4–AP (MNP–AP) and Fe_3O_4–FP (MNP-FP) was collected by filtering, washed to neutral with water, dried at 50°C for 24 h and finally stored for further use [34]. MNLA and MNLFL adsorbents were tested with the magnet and both of them were collected rapidly by the magnet due to the magnetic behavior of them [24].

Preparation of magnetic nanoparticles loaded green tea waste

Magnetite nanoparticles loaded green tea waste (MNLGTW) was synthesized according to the following procedure: $FeCl_3.6H_2O$ (11.68 g) and $FeCl_2.4H_2O$ (4.30 g) were dissolved in 200 mL double distilled water with vigorous stirring at 85ºC. Then, 5.0 g of pretreated green tea waste was added and the mixture was stirred for 30 min. After that, 20 mL of 30%(v/v) NH_3 solution was gradually added to the solution. The color of bulk solution changed from orange to black, immediately. Mixture was stirred at 85ºC for 2 h. The MNLGTW was washed several times with double distilled water and twice with 0.02 mol L^{-1} sodium chloride. The washed MNLGTW was dried under vacuum. MNLGTW adsorbent was tested with the magnet and It is clearly observed that all the MNLGTW were attracted by the magnet, because of the magnetic behavior of the magnetite nanoparticles [31].

Preparation of magnetite nanoparticles loaded peanut husk

Magnetically responsive peanut husk was prepared in a similar way as magnetic sawdust [12]. Three grams of powdered husk in a 50 mL polypropylene centrifuge tube was suspended in 40 mL of methanol and then 6 mL of ferrofluid was added. Water-based ionic- magnetic fluid stabilized with perchloric acid was prepared using a standard procedure [35]. The suspension was mixed on a rotary mixer (Dynal, Norway) for 1 h. The magnetically modified peanut husk particles were then washed twice with methanol and air dried [10] and all of the MNLPH were attracted by the magnet. Loading amount of Fe_3O_4 on 1g of natural

adsorbents modified with magnetite nanoparticles according to EDX were 1.37, 0.84, 1.38 and 1.09 g for Green tea waste,

Peanut husk, Fig leave and Azolla respectively (Fig. 2).

RESULT AND DISCUSSION

Characterization of the MNPs

Characterization of MNLGTW, MNLPH, MNLA,and MNLFL were studied using XRD and SEM. Fig. 3 show the SEM images of the pretreated green tea waste, peanut husk, Azolla, Fig leave and synthesized adsorbents (MNLGTW, MNLPH, MNLA and MNLFL). Images indicated that the surface of natural adsorbents were modified with magnetite nanoparticles and gave it magnetic properties.

The XRD pattern of natural adsorbents and (MNLGTW, MNLPH, MNLA,and MNLFL) are shown in Fig. 4. As the XRD pattern of magnetite loaded nanoparticles shows the typical peaks of Fe_3O_4 can be observed. The results confirm that Fe_3O_4 nanoparticles are successfully impregnated onto natural adsorbents. The typical peaks of magnetite at 2θ= 30.2º, 35.6º, 43.3º and 57.2º are observed that can be assigned to magnetite. XRD patterns for MNLGTW, MNLPH, MNLA and MNLFL include all natural adsorbents and magnetite nanoparticles peaks. The results confirm that natural adsorbents surfaces were loaded with iron oxide nanoparticles.

The spectra of MNLA and MNLFL display a number of absorption peaks, indicating the complicated nature of Azolla and Fig leaves. FT-IR analysis indicated broad band at 3420 cm^{-1}, representing bonded –OH groups. The band observed at about 2850–2920 cm^{-1} could be assigned to the aliphatic C–H group. At wave numbers around 1720 cm^{-1} a shoulder is observed which may be related to the stretching vibrations of carbonyl in carboxyl group. The bands at 1620–1630 cm^{-1} represents the C–O stretching mode conjugate with the NH_2 (amide 1 band) [36]. Absorption bands around 1380 cm^{-1} represent alkyl

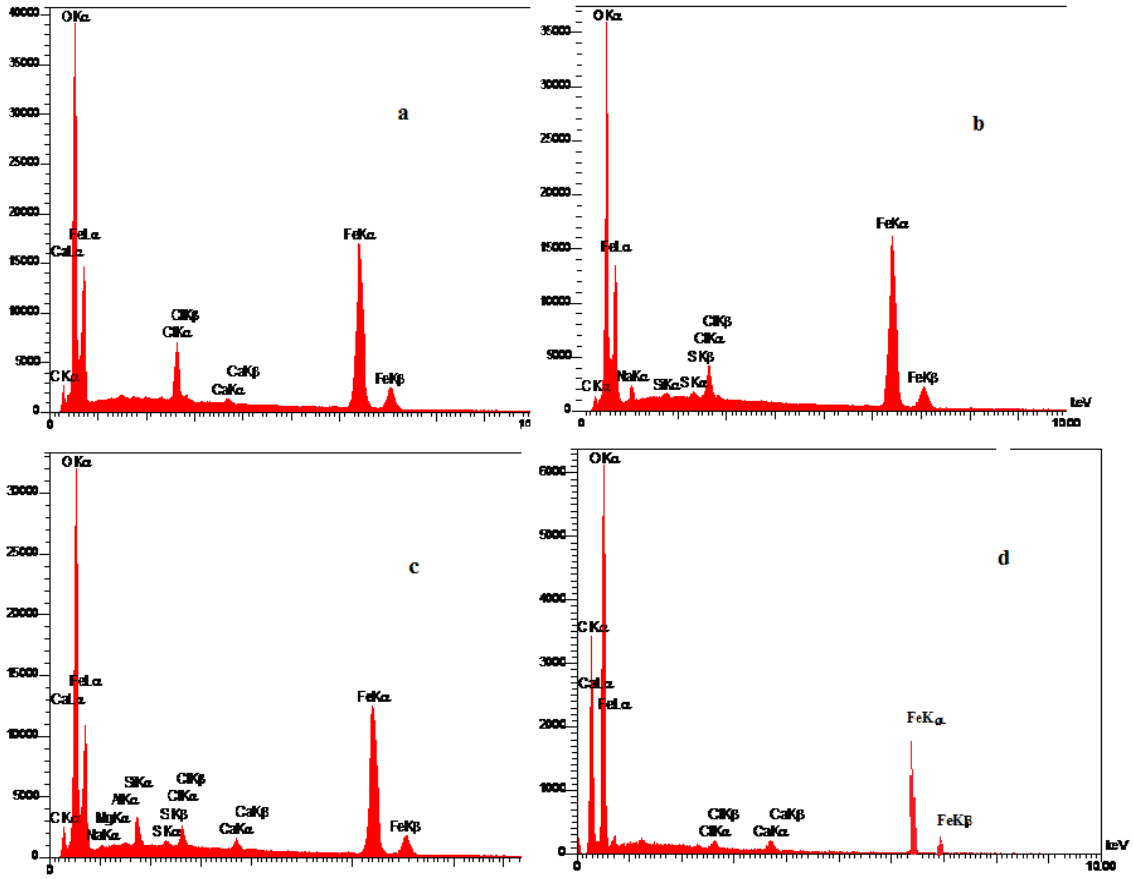

Fig. 2. Energy Dispersive X- ray (EDX) analysis of (a) MNLTW, (b) MNLFL, (c) MNLA (d) MNLPH

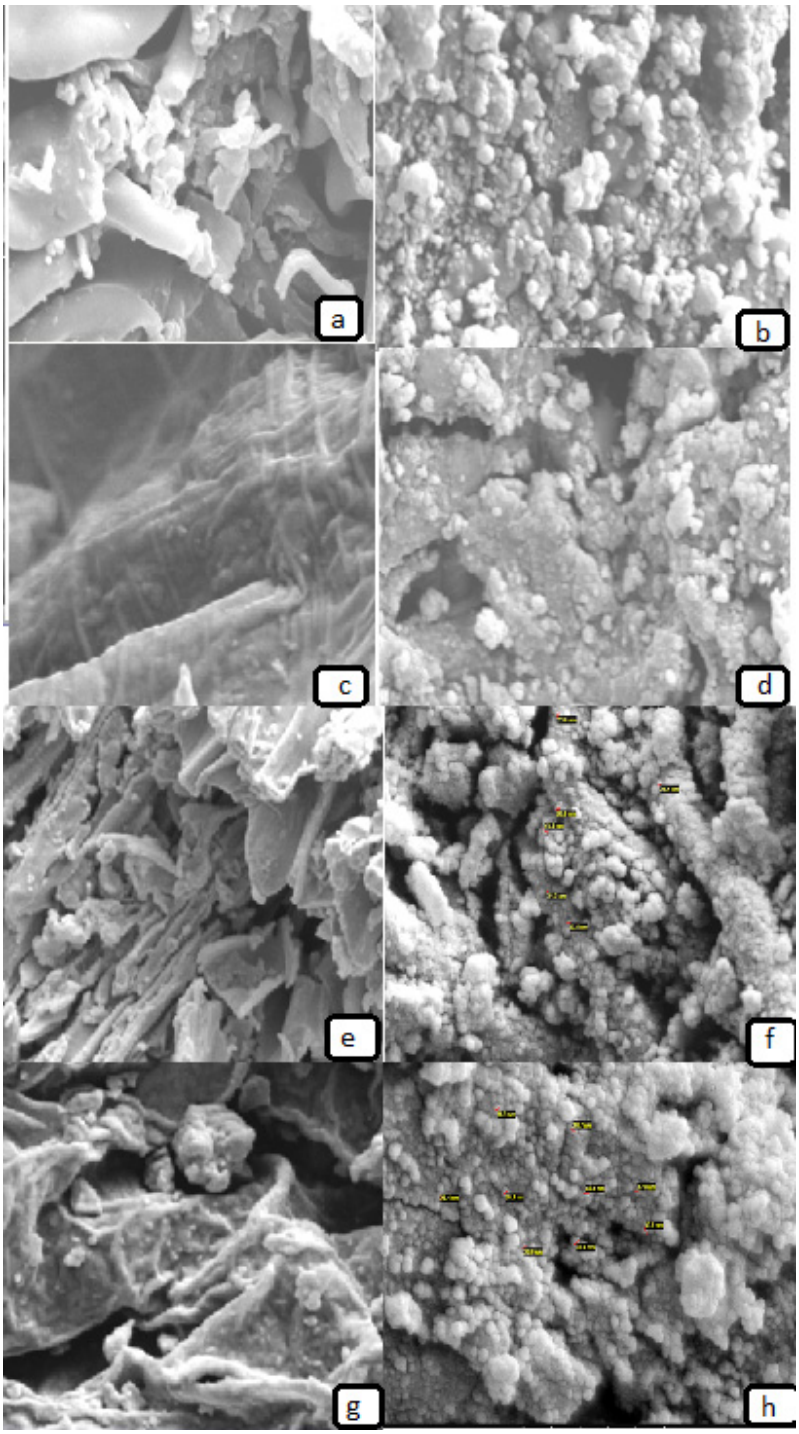

Fig. 3. The SEM image of (a) pretreated green tea waste, (b) MNLTW, (c) pretreated peanut husk and (d) MNLPH, (e) pretreated Fig leaf, (f) MNLFL, (g) pretreated Azolla (h) MNLA

group. The band observed at about 1000–1100 cm^{-1} could be assigned to the aliphatic C–N bond. With comparison, the spectra in Fig. 5 (a to d) shows that there were almost the same functional groups detected on the surface of MNLA, MNLFL and a peak is observed in 588 cm^{-1} that is related to the Fe–O group.

The FT-IR spectra of both modified and unmodified green tea wastes and peanut husk are shown in Fig. 5 (e to h). The spectra display a number

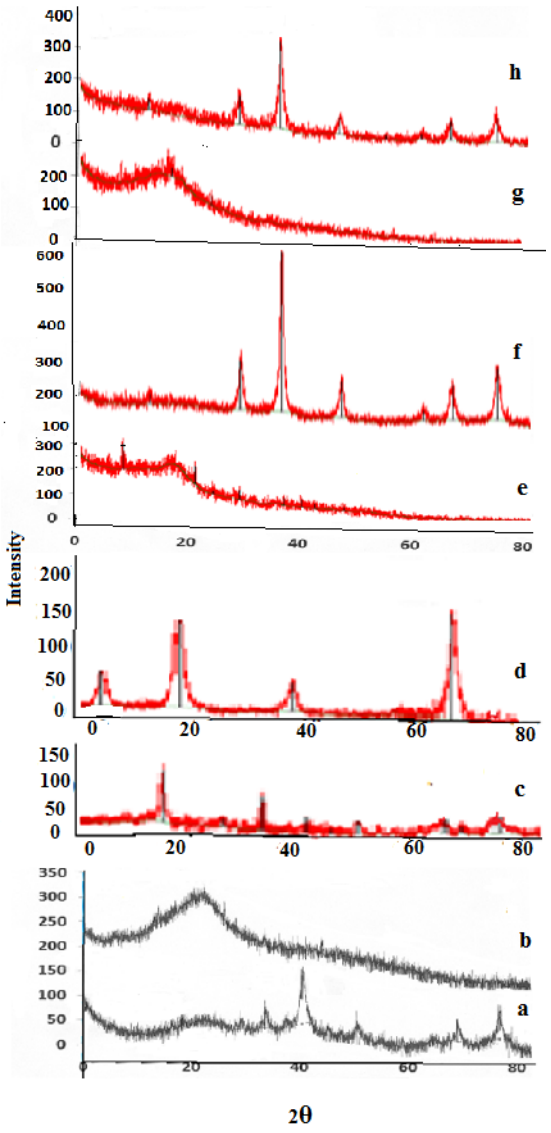

Fig.4. XRD pattern of (a) MNLGTW, (b) pretreated green tea waste, (c) pretreated peanut husk and (d) MNLPH. (e) pretreated Fig leaf, (f) MNLFL, (g) pretreated Azolla and (h) MNLA

of absorption peaks, indicating the complex nature of tea waste and peanut husk. The troughs, due to bonded OH groups, are observed in the range of 3340– 3380 cm^{-1}. The FT-IR spectroscopic analysis indicated broad band's at 3420 cm^{-1}, representing bonded –OH groups. The band observed at about 2920–2850 cm^{-1} could be assigned to the aliphatic C–H group. At wavenumber around 1720 cm^{-1} a shoulder is observed which may be due to the carbonyl stretching of carboxyl. The trough at 1640–1660 cm^{-1} represents the C–O stretching mode conjugate with the NH_2 (amide 1 band) [36, 37]. The peak observed at 1543 and 1520 cm^{-1} corresponds to the secondary amine group. With comparison, the spectra in Fig. 5 (a to h) shows that there were almost the same functional groups detected on the surface of MNLTW, MNLPH and a peak is observed in the Fe–O group at 588 cm^{-1}.

Dye adsorption optimization

In primary experiments,the optical absorption behavior of malachite green at various pHs was studied with measuring the absorbance of MG (4 mg L^{-1}) solutions at 620 nm. Various parameters affecting the removal efficiency of MG were studied and optimized to achieve maximum adsorption efficiency. For optimization studies, 0.03 g of adsorbents (MNLGTW, MNLPH, MNLA,and MNLFL) was added to 20mL solution of MG at different concentrations in a 50 mL beaker. pH of the solution was adjusted to the desired value using 0.1 mol L^{-1} HCl and NaOH and the solution was stirred for 30 min. After MG adsorption; adsorbent was quickly separated from the sample solutions using a super magnet (1.4T). The residual MG concentrations in the supernatant clear solution was determined spectrophotometrically using a calibration curve. The following equation was applied to calculate the dye removal efficiency in the treatment experiments:

$$\text{Dye removal efficiency } \%R = \frac{C_0 - C_t}{C_0} \times 100 \qquad (1)$$

C_o and C_t are the initial and residual concentrations of the dye.

Effect of amount of adsorbent on the MG removal efficiency

The dependence of the adsorption of MG on the amount of adsorbent was studied at room temperature and at optimum pH by varying the adsorbent amount from 0.01–0.05 g in contact with 20 mL solution of 4 mg L^{-1} of MG. Apparently, the percentage removal increased by increasing the number of adsorbents due to the increase in the contact surface of adsorbent with MG and the greater availability of the adsorbents. The adsorption reached a maximum with 0.03 g of the adsorbents. Fig. 6. So this amount of the adsorbents was selected for further works.

It is apparent that by increasing the dose of the adsorbents, the number of sorption sites available for interaction with dye is increased, thereby resulting is in the increased percentage of MG

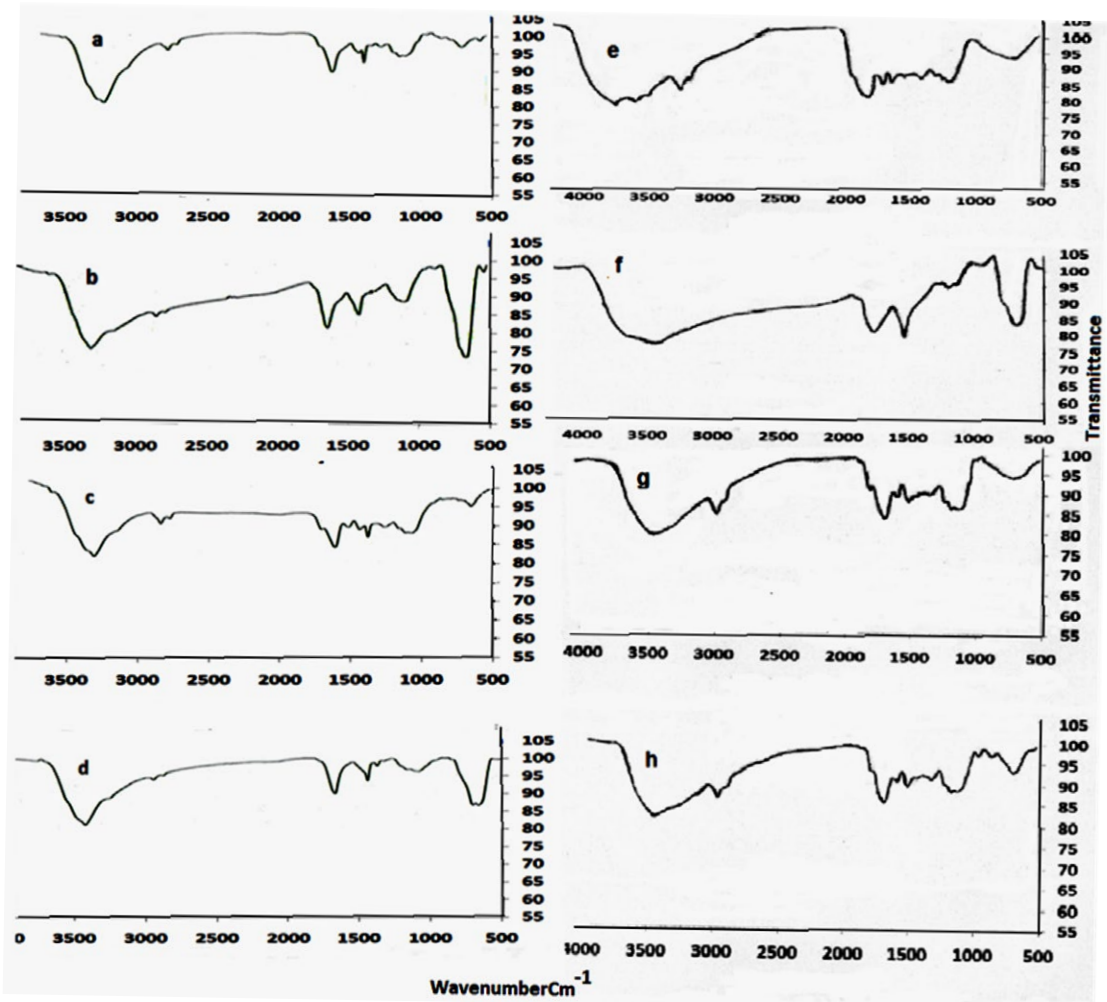

Fig. 5. FT-IR spectra of (a) pretreated Fig leave, (b) MNLFL, (c) pretreated Azolla, (d) MNLA, (e) pretreated tea waste, (f) MNLGTW, (g) pretreated peanut husk and (h) MNLPH

removal from the solution. The decrease in sorbent capacity, that is, the amount of MG sorbed per unit weight of sorbent with increase in adsorbents dose may be attributed to two reasons, The increase in sorbent dose at constant MG concentration and volume will lead to unsaturation of sorption sites through the sorption process and secondly may be due to particulate interaction such as aggregation resulting from high sorbent dose such aggregation would lead to a decrease in total surface area of the sorbent [38].

Effect of contact time on the MG removal efficiency

The effect of contact time on the adsorption of dyes was studied to determine the time taken by adsorbent to remove 4 mg L^{-1} MG solution. The absorbance of the residual solution at λ_{max} was measured at different times. It was observed in Fig. 7 that almost maximum of MG became adsorbed after 30 min for all of adsorbents and this time is enough to reach semi equilibrium conditions. Therefore, agitation time of 30 min was selected for further works.

Effect of pH on the MG removal efficiency

Solution pH influences adsorption process by affecting both aqueous chemistry and surface binding-sites of the adsorbent. The effect of pH on the MG removal efficiency was investigated in the pH range of 3.0–12.0 with a stirring time of 30 min. Fig. 8 shows the removal efficiency of MG as a function of pH. The percent adsorption increased by increasing pH and reached maximum at pH=7-10. The electrical charges on adsorbent materials which is related to the ionization of the polar functional groups on the absorbent surface

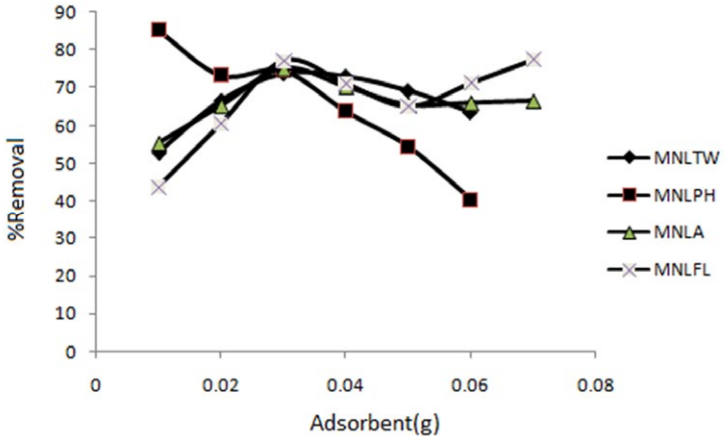

Fig. 6. Effect of amount of adsorbents on the MG removal efficiency (C_{dye} = 4 mg L^{-1}, V = 20 mL)

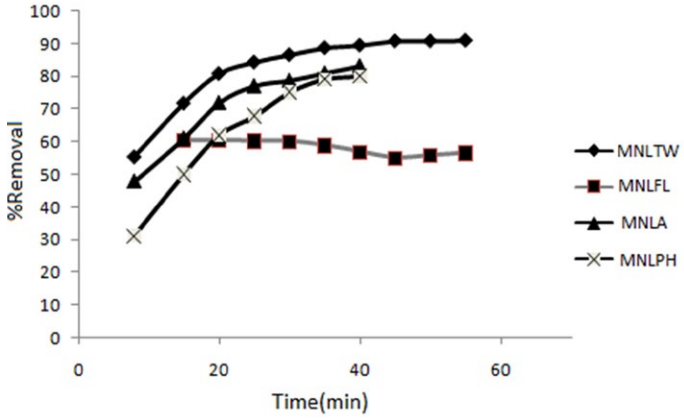

Fig. 7. Effect of contact time on the MG removal (C_{MG} = 4mg L^{-1}, V = 20 mL).

are known to depend on pH. Insoluble cell walls of tea leaves are largely made up of cellulose and hemicelluloses, lignin, condensed tannins and structural proteins. The dominant groups in lignin, tannin or other phenolic compounds are mainly corboxylate, aromatic corboxylate, phenolic hydroxyl and oxyl groups [36]. According to the results from Fig. 8, maximum adsorption of cationic dye takes place at pH 7-10 because in the process of adsorption, at a lower pH the adsorbent surface is positively charged, favoring adsorption on anionic contaminants but MG is a cationic dye, positive charge which occupied the feasible adsorption position competes with dye molecules, resulting in a lower adsorption of dye but in higher pH, the surface of the adsorbent is negatively charged and attraction of the opposite charges is responsible for higher adsorption [39].

Effect of speed of mixing and ionic strength on the MG removal efficiency

The increase in the adsorption rate and adsorption capacity in the case of agitation was on the result of the physical contact between adsorbents and dye. As a result, the adsorbent material gets reduced in size and the adsorption sites are more easily accessible to the adsorbente molecules[40]. The transfer rate of a solute to a particle is affected by liquid film thickness surrounding the particle and the film thickness depends on agitation speed. It was observed that the adsorbed MG by adsorbents increased with the increase in agitation speed in the range of 500 to 2000 RPM. The results showed that percent of removal was maximum at 1500 RPM But at agitation rates higher than 1500 RPM the sorption rate was reduced, indicating that the film thikness has insignificant effect when the agitation

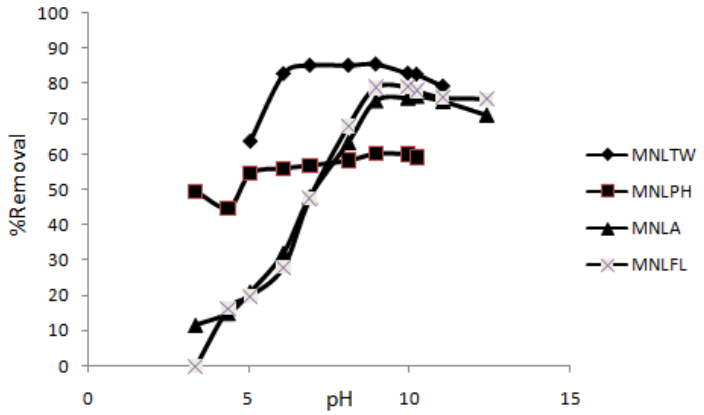

Fig. 8. Effect of PH of solution on the MG removal (C_{MG} =4 mg L^{-1}, V = 20 mL).

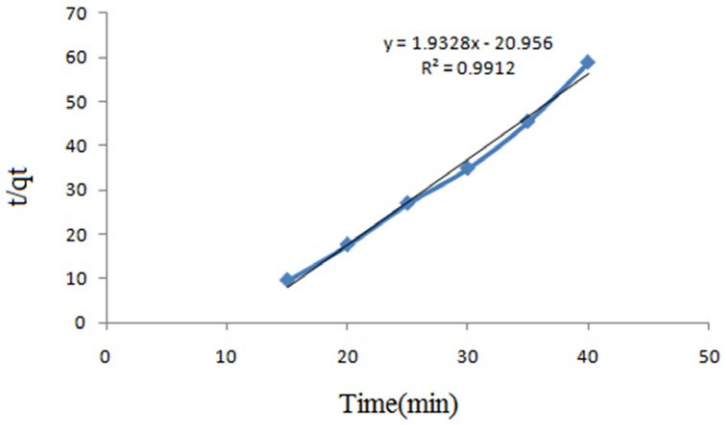

Fig. 9. Fitting of kinetic data to the pseudo-second order kinetic model for MNLFL (C_{MG} = 4 mg L^{-1}, MNLFL= 0.03 g, pH=8)

rate is higher than 1500 RPM, Hence agitation rate of 1500 RPM was selected for all the experiments.

The effect of ionic strength on the MG adsorption was investigated by addition of NaCl in the range of 0–10% (w/v). The results showed that with the increase of the NaCl concentration, the adsorption capacity of adsorbents modified with nanoparticles was increased significantly between 8 to 10% (w/v). The increase in dye removal after NaCl addition can be attributed to an increase in dimerization of dye in solution. A number of intermolecular forces include vander waals forces, ion-dipole forces, and dipole-dipole forces which occur between dye molecules in the solution it has been reported that these forces increased upon the addition of salt to the dye solution [41]. Accordingly, the higher adsorption capacity of dye under these conditions can be attributed to the aggregation of dye molecules induced by the action of salt ions, Salt ions force dye molecules to aggregate, increasing the extent of sorption on the adsorbent[42].

The study of kinetic and adsorption isotherms

The study of kinetics of MG adsorption onto MNLGTW, MNLPH, MNLA and MNLFL adsorbents is required for selecting optimum operating conditions for the full-scale bath processes. The kinetic parameters, which are helpful for the prediction of the adsorption rate, give important information for designing and modeling the adsorption processes. The kinetic data for adsorption onto MNLGTW, MNLPH, MNLA and MNLFL were analyzed using pseudo-first, pseudo-second order and intra-particle diffusion models to find out the adsorption rate expression. The conformity between experimental data and the models predicted values were expressed by the correlation coefficients (R^2, values close to 1), show the influence of time on the dye removal. In

the present study, kinetic studies were performed at various initial dye concentrations 5–500 mg L^{-1} for dye and the solutions were stirred in the time intervals ranged from 0 to 70 min. Then, the clear supernatant solutions were spectrophotometrically measured for residual MG concentration in the solution. Fig. (9-12) show the equilibrium concentrations of malachite green at the adsorption time interval of 0–70 min. The concentration of residual MG in the solution was monitored and the adsorption capacity q_t at time t (mg g^{-1}) was calculated by the following equation:

$$q_t = \frac{(C_0 - C_t) \times V}{W} \quad (2)$$

Where C_o and C_t are the initial and equilibrium concentrations (mg L^{-1}) of MG at a given time t, respectively. Also, V is the solution volume (mL) and w is the weight of the adsorbent (g). The removal rate was very fast during the initial stages of the adsorption processes. The kinetic of adsorption was obtained as a pseudo-second order according to the following equation. The rate of pseudo-second order reaction may be dependent on the amount of solute adsorbed on the surface of adsorbent and the amount adsorbed at equilibrium. The kinetic rate equations for pseudo-second-order reaction can be written as follows:

$$\frac{t}{q_t} = \frac{1}{K_2 q_e^2} + [\frac{1}{q_e}]t \quad (3)$$

Where q_t and q_e, are the value of adsorbed MG at each time and at equilibrium and k_2 (g mg^{-1} min^{-1}). is the pseudo-second-order rate constant. If the second-order kinetic equation is applicable, the plot of t/q_t against t (Eq. (3)) should give a linear

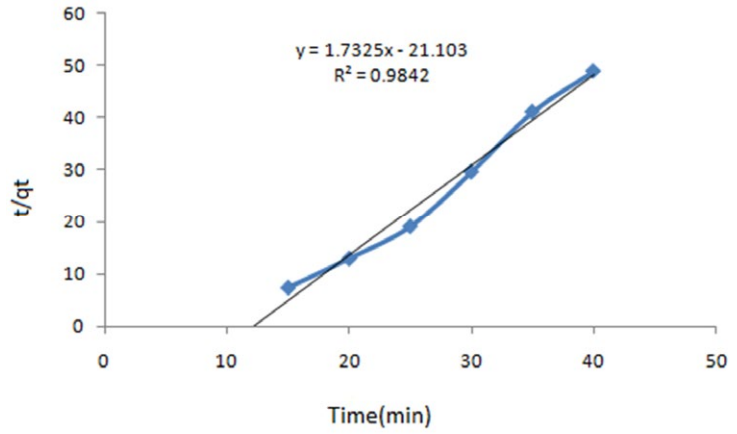

Fig. 10. Fitting of kinetic data to the pseudo-second order kinetic model for MNLA (C_{MG} = 4 mg L^{-1}, MNLA = 0.03 g, pH=8)

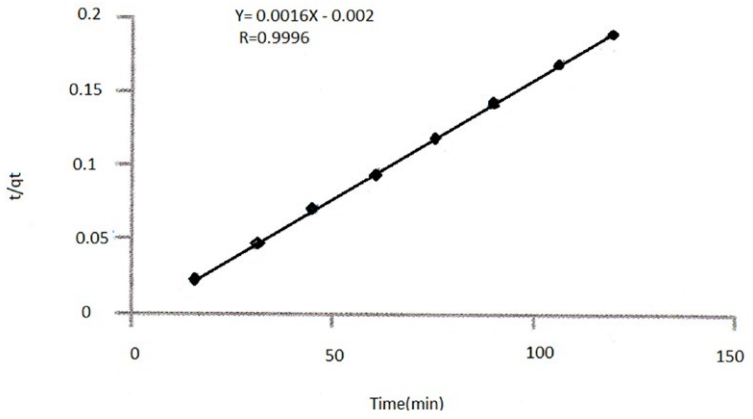

Fig. 11. Fitting of kinetic data to the pseudo-second order kinetic model for MNLPH (C_{MG} = 13 mg L^{-1}, MNLPH= 0.03 g, pH=8)

relationship. The q_e and k_2 can be determined from the slope and intercept of the plot. Fitting of kinetic data to pseudo-second order kinetic model, was shown in Fig. (9 to 12) for MNLFL, MNLA, MNLPH, and MNLGTW.

The best fit of the pseudo-second order kinetic model (R^2 close to 1) (Table 1) in the present system shows the adsorption of MG followed by chemisorptions mechanism via electrostatic attraction.

Equilibrium isotherm equations are used to describe the experimental sorption data. The parameters obtained from the different models provide important information on the sorption mechanisms and the surface properties and affinities of the sorbent. The equilibrium adsorption isotherm was determined using batch studies. 20 mL of the dye solution with various initial dye concentrations in range of 50–500 mg L^{-1}, was poured into a glass bottle. The time required to reach equilibrium as determined in equilibrium studies was 30 min. The amount of dye uptake by the MNLGTW, MNLPH, MNLA and MNLFL, q_e (mg g^{-1}), was obtained by equation(2):

Adsorption data obtained in a concentration range of 50–500 mg L^{-1} were correlated with the following linear forms of Langmuir (Eq. (4)) [43], Freundlich (Eq. (5)) [44], and Tempkin (Eq. (6)) [45] adsorption isotherm models:

Langmuir equation: $$\frac{C_e}{q_e} = \frac{1}{K_l q_{max}} + \frac{1}{q_{max}} c_e \quad (4)$$

Freundlich equation: $$\log q_e = \log K_f + \frac{1}{n} \log c_e \quad (5)$$

Temkin equatin: $$q_e = K_1 . \ln(K_2) + K_1 . \ln(c_e) \quad (6)$$

Where q_e is the equilibrium concentration of dyes on the adsorbent (mg g^{-1}), C_e is the equilibrium concentration of dyes in the solution (mg L^{-1}), q_{max} the monolayer capacity of the adsorbent (mg g^{-1}), K_L the Langmuir constant (L mg^{-1}) and related to the free energy of adsorption, K_F the Freundlich constant (L g^{-1}) and n (dimensionless) is the heterogeneity factor.

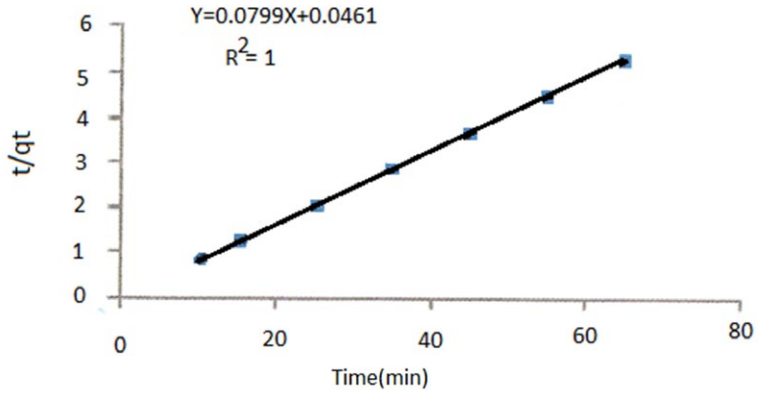

Fig. 12. Fitting of kinetic data to the pseudo-second order kinetic model for MNLGTW (CMG =13 mg L^{-1}, MNLGTW= 0.03 g, pH=8)

Table 1. Comparison of optimum conditions achieved by the proposed sorbent and the other reported sorbents for malachite green removal

Adsorbents	Capacity mg g^{-1}	Reference
Activated chrcoal	0.18	[46]
Clayey soil	78.57	[47]
Polymeric gels	4.9	[48]
Sea shell powder	42.33	[47]
Neem sawdust	4.353	[49]
Bentonite(Cd(oH)2 –NW-AC)[1]	7.72	[50]
	19.0	[51]
Fe3O4@Mel	9.06	[52]
Maghemite nanoparticles	227.3	[53]
Magnetite nanoparticles loaded green tea waste	112.359	This work
Magnetite nanoparticles loaded peanut husk	98.039	This work
Magnetite nanoparticles loaded Azolla	23.1	This work
Magnetite nanoparticles loaded Fig leave	73.2	This work

[1]Cadmium hydroxide nanowires loaded on activated carbon

Table 2. The values of parameters obtained by different kinetic models

Kinetic models	Parameters	MNLFL dye MG	MNLA dye MG	MNLGTW dye MG	MNLPH dye MG
Pseudo-first order	K_1 (min^{-1})	- 0.09	-0.04	1.61×10^{-3}	2.3×10^{-4}
	$q_{e,cal}$ (mg g^{-1})	0.049	0.244	0.161	1.64×10^{-3}
	R_1^2	0.6075	0.1703	0.7394	0.1129
Pseudo-second order	k_2 (g mg^{-1} min^{-1})	0.178	0.142	0.138	1.28×10^{-3}
	$q_{e,cal}$ (mg g^{-1})	0.517	0.5772	12.51	625
	R_2^2	0.9912	0.9842	1	0.9996
Elovich	ß	1.153	0.785	3.524	-0.0607
	α	0.01	0.018	4.88×10^{16}	9.9×10^{19}
	R^2	0.9372	0.9785	0.9416	0.7341

Table 3. The constants values of different adsorption models.

Isotherm models	Parameters	Adsorbent MNLFL Dye MG	MNLA Dye MG	MNLGTW Dye MG	MNLPH Dye MG
Langmuir	q_{max} (mg g^{-1})	73.2	23.1	112.359	98.03
	R^2	0.99	0.9996	0.9504	0.9791
	K_L (L mg^{-1})	0.15	1.54	0.047	0.026
Freundlich	K_F	4.6	2.3	1.89	0.042
	n	3.67	4.47	1.767	9.31
	R^2	0.97	0.8794	0.9303	0.8922
Temkin	K_1	0.42	0.3714	0.3127	0.4373
	R^2	0.93	0.9258	0.8188	0.6846
	K_2	4.6	4.25×10^{2}	1×10^{8}	5×10^{-14}

K_1 is related to the heat of adsorption (L/g) and K_2 is the dimensionless Tempkin isotherm.

In the Langmuir model, a plot of C_e/q_e versus C_e should indicate a straight line of slope

1/ q_{max} and an intercept of $1/(K_L\ q_{max})$. The correlation coefficient ($R^2_{Langmuir}$ = 0:95, $R^2_{Freundlich}$ = 0.93) for green tea waste, ($R^2_{Langmuir}$ = 0:98, $R^2_{Freundlich}$ = 0.89) for Peanut Husk, ($R^2_{Langmuir}$ = 0:99, $R^2_{Freundlich}$ = 0.97) for Fig leave and ($R^2_{Langmuir}$ = 0:99, $R^2_{Freundlich}$ = 0.87) for Azolla showed strong positive evidence on the adsorption of MG onto adsorbents follows the Langmuir isotherm (Table 2). The Langmuir adsorption isotherm assumes that adsorption takes place at specific homogeneouns sites within the adsorbent and it has been used successfully for many adsorption processes of monolayer adsorption.This indicates that the adsorption of MG occurs on a homogenous surface by monolayer adsorption without any interaction between adsorbed ions. The value of Q_{max} for adsorption of MG was obtained from the Langmuir model as 112.359, 98.039, 23.1 and 73.2 mg g^{-1} for MNLGTW, MNLPH, MNLA,and MNLFL, respectively.

CONCLUSION

The sorption of pollutants from aqueous solutions plays a significant role in water pollution control. For this purpose, the utilization of the MNLGTW, MNLPH, MNLA,and MNLFL as efficient adsorbents were successfully carried out to remove the MG dye from samples. The rapid adsorption rate is mainly attributed to the tea leave and peanut husk structure and functional groups on them providing large surface area and good affinity for the facile and fast adsorption of dye molecules. The adsorption followed the pseudo-second order kinetic model, suggesting chemisorption. The fit of the Langmuir model in the present system shows the formation of a monolayer covering of the adsorbate at the outer space of the adsorbent. The MNLGTW, MNLPH, MNLA and MNLFL are synthesized easily. Due to their very high surface areas, high adsorption capacity can be achieved by using magnetic nanoparticles loaded them. The data reported here should be useful for the design and fabrication of an economical treatment process for dye adsorption in industrial effluents. Comparison of optimum conditions achieved by the proposed sorbent and the other reported sorbents for MG removal are in (Table 3).

ACKNOWLEDGMENTS

This research is the result of research project No. 7/36027 dated 1/7/2015 of the Vice-Chancellor of

Research of the University of Guilan. The authors extend their sincere thanks to the University of Guilan for its funding of this research.

CONFLICT OF INTEREST

The authors declare that there is no conflict of interests regarding the publication of this manuscript.

REFERENCES

[1] V.K. Garg, R. Kumar and R. Gupta, Dyes. Pigm., 62, 1 (2004).
[2] S. Srivastava, R. Sinha and D. Roya, Aquat. Toxicol., 66, 319 (2004).
[3] Food standards Australia newzeland Consumer. Chemical in foods., (2005). http://www.foodstandards.gov.au/consumer/chemicals/malachitegreen/Pages/default.aspx
[4] R. Mirzajani and S. Ahmadi, J. Ind. Eng. Chem., 23, 171 (2014).
[5] S. Namrodi, M. Golipor, H. Mirrezai and M. Mazandarani, National conference about planning of environmental protection. (2013).
[6] N. Nashaat, N. Nassar, N. Nedal, G. Vitale and A. Arar, J. Chem. Engin., 93, (2015).
[7] S. Kanchi, Environ. Anal. Chem. (2014).
[8] S. Chakraborty, S. Chowdhury and P.D. Saha, J. Carbohydr. Polym., 86, 1533 (2011).
[9] Y. Liu, X. Sun and B. Li, J. Carbohydr. Polym., 81, 335 (2010).
[10] I. Safarik, M. Safarikova, Phys. Proced., 9, 274 (2010).
[11] I. Safarik, K. Horska, B. Svobodova and M. Safarikova, Eur. Food Res. Technol., 234, 345 (2012).
[12] I. Safarik, P. Lunackova, E. Mosiniewicz-Szablewska, F. Weyda and M. Safarikova, Holzforschung., 61, 247 (2007).
[13] C. Namasivayam and N. Kanchana, Chemosphere., 25, 1691 (1992).
[14] C. Namasivayam, N. Muniasamy, K. Gayatri, M. Rani and K. Ranganathan, Bioresour. Technol., 57, 37 (1996).
[15] T. Robinson, B. Chandran and P. Nigam, Water. Res., 36, 2824 (2002).
[16] O. Serpil and K. Fikret, Environ. Manage., 81, 307 (2006).
[17] Y. Bulut, N. Gozubenli and H. Aydin, Hazard. Mater., 144, 300 (2007).
[18] M.T. Sulak, E. Demirbas and M. Kobya, Bio Tech., 98, 2590 (2006).
[19] A. Mittal, L. Kurup and J. Mittal, Hazard. Mater., 146, 243 (2007).
[20] F. Ovaisi, M. Nikazar and MH. Razagi, National conference about planning of environmental protection, (2012).
[21] W. WU, Q. He and C. Jiang, Nanoscale Res Lett., 3, 397 (2008).
[22] M. Golshekan and SH. Shariati, ACta. Chim., 60, 2, 358 (2013).
[23] M. Manoochehri, SM. Mostashari, and SH. Shariati, Cell. Chem.Tech., 47, 727 (2013).
[24] SH. Shariati, M. Faraji, Y. Yamini and A.A. Rajabi, Else Desal., 270, 160 (2011).
[25] N. Yang, S. Zhu, D. Zhang and S. Xu, Mater. Lett., 62, 645 (2008).
[26] J. Park, K. An, Y. Hwang, J.G. Park, H.J. Noh, J.Y. Kim, J.H. Park, N.M. Hwang and T. Hyeon, Nat. Mater., 3, 891 (2004).
[27] J.H. Jang and H.B. Lim, Microchem., 94, 148 (2010).
[28] N.A. Taha and, E. maghraby, J. Glob. Nest., 17, 25 (2015).
[29] D. Ashoori, S.A. Noorhosseini and S.F. Noorhosseini, Bioscien. IJB., 4, 196 (2014).
[30] Green Tea Processing. How Green Tea is processed. Available at: https://www.o- cha.com/green-tea- processing.html
[31] N. Alizadeh. S. Shariati, N. Besharati, Int. J. Environ. Res., 11,197 (2017).
[32] T.V. Padmesh, K. Vijayaraghavan, G. Sekaran and M. Velan, J. Hazard. Mater., 125, 121 (2005).
[33] H. Benaïssa, Thirteenth International Water Technology Conference IWTC Hurghada Egypt., 13 (2009).
[34] V.K. Gupta and A. Nayak, J. Chem. Eng., 180, 81 (2012).
[35] R. Massart, IEEE. Trans. Magn., 17, 1247 (1981).
[36] P. Panneerselvam, N. Morad and K.A. Tan, Hazard. Mat., 186, 160 (2011).
[37] L.C.A. Oliveira, R.V.R.A. Rios, J.D. Fabris, K. Sapag, V.K. Gargc and R.M. Lago, Appl. Clay. Sci., 22, 169 (2003).
[38] E.N. EI Qada, S.J. Allen and G.M. Walker, Chem. research., 17, 6044 (2006).
[39] G. Zhang and y. Bao, Energy. procedia., 16, 1141 (2011).
[40] K. Kusmierek and A. Swiatkowski, Reac kinet mech cat., 116, 261 (2015).
[41] G. Alberghina, R. Bianchini, M. Fichera and S. Fisichella, Dyes. Pig., 46, 129 (2000).
[42] J. German Heins and M. Flury, Geoderma., 97, 87 (2000).
[43] I. Langmuir, Am Chem. Soc., 40, 1361 (1918).
[44] H.M.F. Freundlich, Z. Phys. Chem., 57, 385 (1906).
[45] M.J. Tempkin and V. Pyzhev, Acta. PhysioChim., 12, 271 (1940).
[46] M.J. Iqbal and M.N. Ashiq, J. Hazard.Mater., 139, 57 (2007).
[47] P. Saha, S.h. Chowdhury, S. Gupta and I. Kumar, Chem Eng J., 165, 874 (2010).
[48] M.A. Malana, S. Ijaz and M.N. Ashiq, Desalination., 263, 249 (2010).
[49] S.D. Khattri and M.K. Singh, J. Hazard. Mater., 167, 1089 (2009).
[50] S.S. Tahir and N. Rauf, Chemosphere., 63, 1842 (2006).
[51] M. Ghaedi and N. Mosallanejad, J. Ind. Eng. Chem., 20, 1085 (2014).
[52] R. Mirzajani and S. Ahmadi, J. Ind. Eng. Chem., 23, 171 (2015).
[53] A. Afkhami, R. Moosavi and T. Madrakian, Talanta., 82, 785 (2010).